Journal of Applied Fluid Mechanics, Vol. 9, No. 2, pp. 741-749, 2016.
Available online at www.jafmonline.net, ISSN 1735-3572, EISSN 1735-3645.
DOI: 10.18869/acadpub.jafm.68.225.21441

Soret Convection in a Shallow Porous Cavity under a Magnetic Field and Submitted to Uniform Fluxes of Heat and Mass

M. Bourich[1], M. Hasnaoui[2†], A. Amahmid[2], M. Er-Raki[3], A. Lagra[1]and M. Mamou[4]

[1]*National School of Applied Sciences, University Cadi Ayyad, Marrakech, Morocco*
[2]*FSSM, LMFE, Unit affiliated to CNRST (URA 27), University Cadi Ayyad,Marrakech, Morocco*
[3]*High School of Technology, University Cadi Ayyad, Essaouira, Morocco*
[4]*AL/IAR, National Research Council Canada, Ottawa, Ontario, K1A 0R6, Canada*

†*Corresponding Author Email: hasnaoui@uca.ma*

(Received October 27, 2013; accepted July 29, 2015)

ABSTRACT

Combined effects of magnetic field and thermodiffusion (Soret effect) on natural convection within an electrically conducting binary mixture, confined in a horizontal sparsely packed porous enclosure subjected to uniform fluxes of heat and mass, is studied analytically and numerically. In the limit of a shallow enclosure, an analytical solution is derived using the parallel flow approximation. The approximate analytical solution is validated against the numerical solution of the full governing equations using a finite difference method. Interesting flow bifurcation phenomena are obtained herein and discussed. The linear stability theory and the parallel flow concept are used to determine explicitly the thresholds for the onset of stationary, subcritical and oscillatory convections as functions of the governing parameters. The obtained results showed the existence of different regions in the (N, Le) plane that correspond to different parallel flow behaviors. The number and the locations of these regions depend on the Soret parameter. The existence of a codimension-2 point is demonstrated. The effects of the Hartmann number on the fluid flow intensity and heat and mass transfer characteristics are also discussed.

Keywords: Soret convection; Magnetic field; Linear stability; Thresholds of instabilities; Stability diagram.

NOMENCLATURE

A_r	aspect ratio of the porous matrix, L'/H'
B	strength of the magnetic field
Da	Darcy number,K/H'^2
j'	constant mass flux per unit area
Ha	Hartmann number,$B\sqrt{\kappa K/\mu}$
K	permeability of the porous medium
Le	Lewis number,α/D
N	buoyancy ratio
Nu	Nusselt number
M	soret parameter
q'	constant heat flux per unit area
R_T	thermal Darcy-Rayleigh number, $g\beta_T K\Delta T' H'/(\alpha\upsilon)$
R_{TC}	critical thermal Rayleigh number
S	dimensionless concentration
Sh	Sherwood number
t	dimensionless time
T	dimensionless temperature
$\Delta T'$	characteristic difference of temperature
(u,v)	dimensionless velocities in (x,y) directions
(x,y)	dimensionless coordinates
α	thermal diffusivity of the porous medium,$\lambda/(\rho C)_f$
β_T	thermal expansion coefficient
ε	normalized porosity,ε'/σ
υ	kinematic viscosity of the fluid
μ	dynamic viscosity of the fluid
κ	electrical conductivity of the fluid
ψ	dimensionless stream function
ζ	dimensionless vorticity

Subscripts

C	critical value

max	maximum value

Superscripts

$Hopf$	hopf's bifurcation
sub	subcritical
sup	supercritical

1. INTRODCUTION

The problem of natural convection of an electrically conducting fluid under a magnetic field has been the subject of numerous recent studies. This interest stems from the implication of the phenomenon in many engineering applications involving convective flows under magnetic fields such as in metallurgy, in general, and in crystal growth, in particular. The magnetic force induced by the applied magnetic field may be used as a supplementary force, in addition to the gravitational acceleration force, to control the convective flow behaviour (Braithwaite *et al*. 1991; Jana *et al*. 2006). The magnetizing force occurs in both electrically conducting fluids (liquid metals) and electrically non-conducting fluids (the diamagnetic and paramagnetic fluids).

The literature review shows that natural convection under a magnetic field in different flow geometries has been the object of numerous studies. Now, it is well known that the interaction between a strong magnetic field and the thermal natural convection could lead to suppression or to a substantial reduction of the convection flow intensity followed by an important decrease of heat transfer rate (Kaneda *et al*. 2005;Xu*et al*. 2006;Ece and Büyük 2005). Thermodiffusion, also called Soret effect, is observed in a large number of systems, such as ferrofluids (magnetic colloids) and systems where magnetic nanograins are dispersed in a carrying fluid. Different techniques were used in experiments to measure the Soret coefficient. Separation in thermodiffusion columns (Blums *et al*. 1998), optically-induced thermal grating in thin ferrofluid layers (Mezulis and Blums 2003) and Z-scan systems (Alvesa *et al*. 2005), are some of techniques already used for flow visualization. Experimental results (Blums 2005) on magnetic Soret effect, considering various ferrofluids (magnetite in tetradecane (Blums *et al*. 1997), Mn–Zn ferrite in tetradecane (Blums*et al*. 1998), magnetite in toluene (Mezulis and Blums 2003) show that the combined magnetic and Soret effect in a ferrofluid layer has an influence on the Soret coefficient. In addition, the Soret effect may play a significant role in the problem of long term stability of ferrofluids, especially when the fluid is used as a heat transport medium (i.e. application of temperature gradients), the thermophoretic transfer of particles affected strongly the stability of the ferrofluids (Völker *et al*. 2004;Odenbach and Völker 2005). The thermodiffusion process of magnetic particles in a ferrofluid under the influence of a magnetic field was studied by Völker and Odenbach (2005a-b) to determine the Soret coefficient. The authors reported that the so-called magnetic Soret coefficient was theoretically predicted to be two to three orders of magnitude smaller than the conventional Soret coefficient. In contrast, previous experiments (Blums *et al*. 1998) had qualitatively shown that the magnetic Soret effect was seen to be much higher than the theoretical predictions. This discrepancy was attributed by the authors to the measurement disturbance in those experiments, caused by the influence of buoyancy driven convection under magnetic field. The influence of Soret and Dufour effects on MHD buoyancy-driven heat and mass transfer over a stretching sheet in a saturated porous medium was investigated numerically by Pal and Mondal (2013). The effects of various physical parameters on the dimensionless velocity, temperature and concentration profiles were depicted graphically and analyzed in detail. Gangadhar (2013) studied hydro-magnetic mixed convection heat and mass transfer over a vertical plate subjected to convective heat exchange with its surrounding in the presence of chemical reaction. It was found that the local skin-friction coefficient, local heat and mass transfer rates at the plate surface increase with an increase in intensity of magnetic field, buoyancy forces, convective heat exchange parameter, Soret number, Eckert number, Dufour number and chemical reaction parameter. Gaikwad and Kamble (2014) performed a linear stability analysis of double diffusive convection in a horizontal sparsely packed rotating anisotropic porous layer in the presence of Soret effect. Their results showed that the mechanical anisotropy parameter has a stabilizing effect on stationary and oscillatory convection. Recently, Pal and Mondal (2014) studied Soret-Dufour effects on hydromagnetic non-Darcy convective-radiative heat and mass transfer over a stretching sheet in porous medium with viscous dissipation and Ohmic heating.Important features of flow and heat and mass transfer characteristicswere analyzed and discussed for different values of physical parameters. Their numerical results revealed that the magnetic field and inertia coefficient reduce the skin friction but reverse effects are seen on local Nusselt number.

The present study focuses on the examination of the combined effects of a magnetic field and Soret diffusion on natural convection within an electrically conducting binary mixture confined in a horizontal sparsely packed porous enclosure subjected to uniform fluxes of heat and mass. The thresholds for the onset of subcritical, oscillatory and stationary convections are obtained explicitly as functions of the governing parameters. Effects of the Hartmann number on the fluid flow intensity and heat and mass transfer characteristics are discussed.

2. GOVERNING EQUATIONS

The studied configuration (Fig. 1) is a two-dimensional homogeneous horizontal porous layer

of length, L', and height, H', having adiabatic and impermeable short boundaries while its long horizontal walls are subject to uniform fluxes of heat,q', and mass, j'. A magnetic field of strength B is applied vertically. The porous medium is assumed isotropic, homogeneous and saturated with an electrically conducting binary fluid mixture.

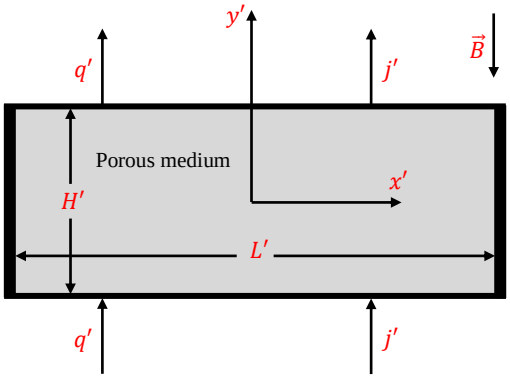

Fig. 1.Schematic diagram of the studied configuration.

The Brinkman-extended Darcy model is adopted and the diluted binary solution that saturates the porous matrix is modeled as a Boussinesq incompressible fluid. The Joule heating of the fluid and the effect of the viscous dissipation are neglected and the magnetic Reynolds number is considered to be small enough so that the induced magnetic field can be neglected compared to the applied one (Shercliff 1965). In addition, there is no electrical field so the Hall effect is neglected. Using the vorticity-stream function formulation, the dimensionless governing equations are stated as follows:

$$\eta\frac{\partial\zeta}{\partial t}+\zeta+Ha^2\frac{\partial^2\psi}{\partial y^2} = Da\nabla^2\zeta - R_T\left(\frac{\partial T}{\partial x}+N\frac{\partial S}{\partial x}\right) \quad (1)$$

$$\frac{\partial T}{\partial t}+u\frac{\partial T}{\partial x}+v\frac{\partial T}{\partial y}=\nabla^2 T \quad (2)$$

$$\varepsilon\frac{\partial S}{\partial t}+u\frac{\partial S}{\partial x}+v\frac{\partial S}{\partial y}=\frac{1}{Le}(\nabla^2 S+M\nabla^2 T) \quad (3)$$

$$\nabla^2\psi=-\zeta \quad (4)$$

$$u=\frac{\partial\psi}{\partial y}\ ,\quad v=-\frac{\partial\psi}{\partial x} \quad (5)$$

The parameterηrepresents the porous medium acceleration coefficient. The hydrodynamic, thermal and concentration boundary conditions associated to the present problem are:

$$x=\pm\tfrac{A_r}{2}\ :\ \psi=0\ ,\ \tfrac{\partial T}{\partial x}=0\ ,\ \tfrac{\partial S}{\partial x}=0 \quad (6)$$

$$x=\pm 1/2\ :\ \psi=0\ ,\frac{\partial T}{\partial y}=-1\ ,\frac{\partial S}{\partial y}=-1+M \quad (7)$$

3. NUMERICAL SOLUTION

The numerical solution of the full governing equations was obtained by using the finite difference method described in Bourich *et al.* (2004).The vorticity, temperature and concentration equations, Eqs.(1)-(3), were solved iteratively in a time accurate mode using the alternating direction implicit method. At the boundaries, the values of the vorticity were calculated using the Wood's relation (Roache 1982). Nodal values of the stream function were obtained, from Eq. (4), via a point successive-over-relaxation method. For large aspect ratio enclosures, a non-uniform grid was used in the horizontal direction to capture the flow details near the enclosure end walls. A non-uniform grid was also used in the y-direction. The results reported in this paper were obtained with a grid of 121×61 for$A_r=4$ and 201×81for $A_r\geq 8$.

The fundamental character of the parallel flow assumption, based on the fact that the flow is parallel in the core of the cavity and linearly stratified. This parallel flow concept was verified numerically by solving the full governing equations. The analytical solution, although valid for a shallow cavity, allows for a rapid parametric study that helps to better understand the flow behavior and heat and mass transfer characteristics that are similar to those observed in confined cavities.

4. PARALLEL FLOW CONCEPT

For shallow enclosures, using the parallel flow assumption (Cormack *et al.* 1974; Mamou *et al.* 2001), a set of ordinary differential equations are obtained for which the solution is developed as follows:

$$\psi(y)=\psi_0\frac{H(y)}{H(0)} \quad (8)$$

$$T(x,y)=C_T x-y+C_T\psi_0\frac{K(y)}{K(0)} \quad (9)$$

$$S(x,y)=C_S x+(M-1)y+\psi_0(LeC_S-MC_T)\frac{K(y)}{K(0)} \quad (10)$$

with

$$\left.\begin{aligned}H(y)&=\frac{cosh(\Omega y)-cosh(\Omega/2)}{\Omega sinh(\Omega/2)}-y^2+\frac{1}{4}\\ K(y)&=\frac{sinh(\Omega y)-\Omega y cosh(\Omega/2)}{\Omega^2 sinh(\Omega/2)}-\frac{y^3}{3}+\frac{y}{4}\end{aligned}\right\} \quad (11)$$

The expressions of C_T and $C_S$were determined by performing thermal and solutal balances at any porous layer cross-section. This yields:

$$C_T=-\frac{A\psi_n}{1+B{\psi_n}^2} \quad (12)$$

$$C_S = \frac{(1-M)LeA\psi_n}{1+B{\psi_n}^2} + \frac{MA\psi_n(1-BLe{\psi_n}^2)}{(1+B{\psi_n}^2)(1+BLe^2{\psi_n}^2)} \quad (13)$$

with

$$A(Da) = -\frac{2}{f(\Omega)} + \frac{1}{\Omega^2} + \frac{1}{12}\ ;\ \Omega = \sqrt{(1+Ha^2)/Da}$$

$$B(Da) = \frac{6}{f(\Omega)^2} + \frac{1}{\Omega^2 f(\Omega)} - \frac{1}{3f(\Omega)} - \frac{1}{8\Omega^2} - \frac{2}{\Omega^4} + \frac{1}{120}$$

$$f(\Omega) = 4\Omega\tanh(\Omega/2) \quad ; \quad \psi_n = -2\psi_0/H(0)$$

$$\psi_0 = H(0)(C_T + NC_S)R_T/[2(1+Ha^2)]$$

The Nusselt and Sherwood numbers are given by the flowing expressions:

$$Nu = \frac{1}{T(x,-1/2) - T(x,1/2)} = \frac{1+B{\psi_n}^2}{1+(B-A^2){\psi_n}^2} \quad (14)$$

$$Sh^{-1} = S(x,-1/2) - S(x,1/2) = (1-M)\frac{(1+(B-A^2)Le^2{\psi_n}^2)}{1+BLe^2{\psi_n}^2} + M\frac{(1+Le)A^2{\psi_n}^2}{(1+B{\psi_n}^2)(1+BLe^2{\psi_n}^2)} \quad (15)$$

5. FLOW BEHAVIOR ANALYSIS

The parallel flow solution is valid as long as the flow remains steady. Thus, we expect that the analytical solution could be unstable for large Rayleigh numbers (Mamou *et al*. 2001) and near criticalities, where oscillatory convective flows are a common occurrence. The range of the solution validity may be delineated by performing a linear stability analysis of the developed flow.

By combining the expressions of C_T and C_S with the equation of ψ_0, one obtains a fifth-order polynomial equation in terms of ψ_0, for which the solution is $\psi_0 = 0$ (trivial solution) and:

$$\psi_0 = \pm\frac{1}{2H(0)Le\sqrt{2B(Da)}}[-b \pm \sqrt{b^2-4Le^2c}]^{1/2} \quad (16)$$

with $b = 1 + Le^2 - \frac{Le(Le+N)R_T^0}{1+Ha^2}$

and $c = 1 - \frac{[1+NLe-(1+Le)NM]R_T^0}{1+Ha^2}$

Here the parameter $R_T^0 = R_T/R^{sup}$ is the normalized Rayleigh number, with $R^{sup} = 1/A(Da)$. From a mathematical point of view, the solution given by Eq. (16) may exhibit two types of bifurcations due to the presence of the two embedded square roots in the expression of ψ_0. These parallel flow solutions exist only when the following conditions are satisfied $-b \pm \sqrt{b^2-4Le^2c} > 0$ and $b^2 - 4Le^2c > 0$. According to these conditions, the (N, Le) plane can be divided into different regions with specific behaviors. The number and the extent of these regions depend on whether $M \le 0, 0 \le M < 1$ or $M \ge 1$. Up to five regions are identified in Fig. 2(a)-(c). In the first region, the parallel flow is not possible. In the second and third regions the only possible flow type is supercritical. However, in the fourth and fifth regions both subcritical and supercritical convections are possible. The supercritical Rayleigh number characterizing the transition from the rest state to the convective regime occurs at zero flow amplitude; its expression is given by:

$$R_{TC}^{sup} = \frac{(1+Ha^2)R^{sup}}{(1+NLe-(1+Le)NM)} \quad (17)$$

The subcritical threshold which occurs through finite amplitude convection at a saddle node point is obtained by solving $b^2 - 4Le^2c = 0$ for R_{TC}^{sub}:

$$R_{TC}^{sub} = (1+Le)(1+Ha^2)f(N,Le,M)R^{sup} \quad (18)$$

with

$$f = \frac{\left[\sqrt{Le(Le+NM-1)} + \sqrt{N(1+Le(M-1))}\right]^2}{Le(Le+N)^2}$$

The parallel flow assumption is based on a steady state flow analysis, and thus the parallel flow approach could not be used to predict the onset of over stabilities. To complete the present study, a linear stability analysis is performed to analyze the rest state stability below the threshold of stationary convection. It can be seen from Figs. 2(a)-(c) that for $M > 0$, the onset of the convective flow via a subcritical bifurcation is possible even for small values of the Lewis number. Furthermore, for $0 < M < 1$ the subcritical convection exists for positive or negative values of N, dependently on the Lewis number. In fact for $Le < Le^*$, the subcritical convection exists for $N > 0$ provided that $Le > 1/(1-M)$, and also for $N < 0$ when $Le < 1/(1-M)$. The expression of Le^* is determined analytically as:

$$Le^* = \frac{M}{3(1-M)} + \sqrt[3]{-\frac{q}{2} + \sqrt{\left(\frac{p}{3}\right)^3 + \left(\frac{q}{2}\right)^2}} + \sqrt[3]{-\frac{q}{2} - \sqrt{\left(\frac{p}{3}\right)^3 + \left(\frac{q}{2}\right)^2}}$$

with $p = \frac{M(2M-3)}{3(M-1)^2}$

and $q = \dfrac{20M^3 - 45M^2 + 27M}{27(M-1)^3}$

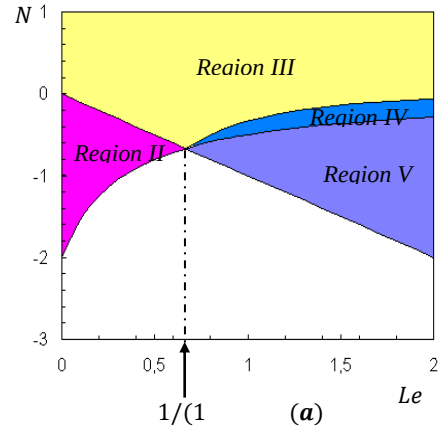

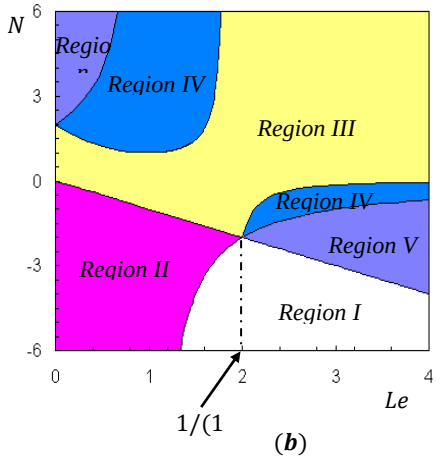

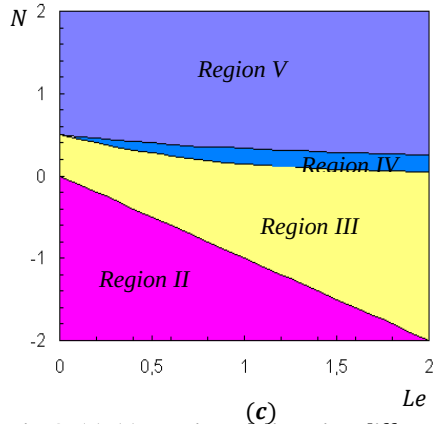

Fig. 2. (a)-(c): Regions delineating different flow regimesfor (a) $M = -0.5$, (b) $M = 0.5$ and (c) $M = 2$.

Finally, in the range $Le^* < Le < 1/(1-M)$, the subcritical convection does not exist. It is to point out that, in the absence of the external magnetic field, the same regions were identified in the $N - Le$ plane (Bourich*et al*. 2003).

The results corresponding to Darcy porous and pure fluid media can be obtained from the Brinkman model as limiting cases:

5.1 Case of Darcy Porous Medium

For $Da << 1$, the expressions ofψ, T, S, C_T, C_S, ψ_0 , Nu and Sh reduce to :

$$\psi(y) = \psi_0(1 - 4y^2) \tag{19}$$

$$T(x,y) = C_T x - y - C_T\psi_0\left(\frac{4}{3}y^3 - y\right) \tag{20}$$

$$S(x,y) = C_S x + (M-1)y$$
$$-\psi_0(LeC_S - MC_T)\left(\frac{4}{3}y^3 - y\right) \tag{21}$$

$$\left.\begin{aligned} C_T &= \frac{10\psi_0}{15 + 8{\psi_0}^2} \\ C_S &= \frac{10(1-M)Le\psi_0}{15 + 8Le^2{\psi_0}^2} \\ &- \frac{10M\psi_0(15 - 8Le{\psi_0}^2)}{(15 + 8{\psi_0}^2)(15 + 8Le^2{\psi_0}^2)} \end{aligned}\right\} \tag{22}$$

$$\psi_0 = \pm\frac{1}{8\sqrt{2}Le}\left(-b \pm \sqrt{b^2 - 4Le^2c}\right)^{1/2} \tag{23}$$

with

$$\begin{cases} b = 120(1 + Le^2) - 10Le(Le + N)\dfrac{R_T}{1 + Ha^2} \\ c = 14400 - 1200[1 + NLe - (1 + Le)NM]\dfrac{R_T}{1 + Ha^2} \end{cases}$$

$$\begin{cases} Nu = \dfrac{3(15 + 8{\psi_0}^2)}{45 + 4{\psi_0}^2} \\ Sh = \left[\begin{aligned} &(1-M)\frac{45 + 4Le^2{\psi_0}^2}{3(15 + 8Le^2{\psi_0}^2)} \\ &+ \frac{800MLe{\psi_0}^2}{(15 + 8{\psi_0}^2)(15 + 8Le^2{\psi_0}^2)} \end{aligned}\right]^{-1} \end{cases} \tag{24}$$

For this limit, the thresholds of convection are obtained from Eqs. (17)-(18) as:

$$R_{TC}^{sup} = \frac{12(1 + Ha^2)}{(1 + NLe - (1 + Le)NM)} \tag{25}$$

$$R_{TC}^{sub} = 12(1 + Ha^2)(1 + Le)f(N, Le, M) \tag{26}$$

5.2 Case of Pure Fluid Medium

For $Da >> 1$, the expressions of ψ, T, S, Nu and Sh reduce to :

$$\psi(y) = \psi_0(4y^2 - 1)^2 \tag{27}$$

$$T(x,y) = C_T x - y$$
$$-C_T\psi_0\left(\frac{16}{5}y^5 - \frac{8}{3}y^3 + y\right) \tag{28}$$

$$S(x,y) = C_S x + (M-1)y$$
$$-\psi_0(LeC_S - MC_T)\left(\frac{16}{5}y^5 - \frac{8}{3}y^3 + y\right) \tag{29}$$

$$\begin{cases} Nu = 10\dfrac{1 + f(\psi(0))}{10 + 3f(\psi(0))} \\ Sh = \left[\begin{aligned} &\frac{1 - M}{Sh(M=0)} \\ &+ \frac{7M(1 + Le)f(\psi(0))}{10[1 + f(\psi(0))][1 + Le^2 f(\psi(0))]} \end{aligned}\right]^{-1} \end{cases} \tag{30}$$

with

$$\begin{cases} Sh(M=0) = 10\dfrac{1+f(\psi(0))}{10+3f(\psi(0))} \\ f(\psi(0)) = \dfrac{1}{70}\left(\dfrac{16\psi(0)}{3}\right)^2 \end{cases} \quad (31)$$

For this limit, the thresholds of convection are obtained from Eqs. (17)-(18) as:

$$R_{TC}^{sup} = \frac{720(1+Ha^2)}{(1+NLe-(1+Le)NM)} \quad (32)$$

$$R_{TC}^{sub} = 720(1+Ha^2)(1+Le)f(N,Le,M) \quad (33)$$

6. LINEAR STABILITY ANALYSIS

In the development of the linear stability analysis, the solution is decomposed into a rest state solution and a perturbation, which yields

$$\left.\begin{array}{l} \psi = 0 + e^{pt}\psi_0 F(x,y) \\ T = -y + e^{pt}\theta_0 G(x,y) \\ S = (M-1)y + e^{pt}\varphi_0 G(x,y) \end{array}\right\} \quad (34)$$

Whereψ, θ and φ are two-dimensional perturbation profiles and p is the growth rate. The corresponding boundary conditions are:

$$\psi = \frac{\partial F}{\partial n} = \frac{\partial G}{\partial n} = 0 \quad (35)$$

on all boundaries, where n is the boundary outward normal vector. The linear governing equations are obtained as follows:

$$\left.\begin{array}{l} (\eta+1)\psi_0\nabla^2 F + Ha^2\psi_0\dfrac{\partial^2 F}{\partial y^2} = Da\psi_0\nabla^4 F \\ \qquad -R_T\left(\theta_0\dfrac{\partial G}{\partial x} + N\varphi_0\dfrac{\partial G}{\partial x}\right) \\ p\theta_0 G + \psi_0\dfrac{\partial F}{\partial x} = \theta_0\nabla^2 G \\ \varepsilon Le p\varphi_0 G + Le\psi_0\dfrac{\partial F}{\partial x} = \varphi_0\nabla^2 G + M\theta_0\nabla^2 G \end{array}\right\} \quad (36)$$

Generally, the solution of the perturbed equations (Eq. (36)) is not possible analytically. However, in the case of enclosures with large aspect ratios, the analytical solution of these equations is possible. At the onset of convection, the amplitudes of ψ, θ and $\varphi$are very small which means that terms with higher order than one (non linear terms) can be neglected. After mathematical developments, the obtained equation is as follows:

$$(1+Ha^2)(1+p)(1+\varepsilon Le p) = R_T^0[p[\varepsilon Le + NLe(1-M)] + 1 + NLe - NMLe - NM] \quad (37)$$

6.1 Onset of Stationary Convection

The threshold of stationary convection is obtained from Eq. (37) with $p = 0$, which leads to:

$$R_{TC}^{sup} = \frac{(1+Ha^2)R^{sup}}{(1+NLe-(1+Le)NM)} \quad (38)$$

This expression is the same as that given by Eq. (17) and predicted by the parallel flow solution.

6.2 Onset of Oscillatory Convection

The threshold for the onset of oscillatory convection (Hopf's bifurcation) is obtained when the real part of the eigenvalue $p = p_r + i\omega$ changes from a negative to a positive value. For a shallow porous enclosure with an infinite aspect ratio, the onset of Hopf's bifurcation is obtained when$p_r = 0$. Introducing this condition in Eq. (37) and knowing that$\omega \neq 0$, the threshold of Hopf's bifurcation can be obtained as:

$$R_{TC}^{Hopf} = \frac{(1+Ha^2)(\varepsilon Le+1)}{\varepsilon Le + (1-M)NLe}R^{sup} \quad (39)$$

From Eq. (39), it is clear to deduce that the occurrence of the oscillatory flow depends not only on Le, N, Ha, Da and M (as it is the case forR_{TC}^{sup}andR_{TC}^{sub}) but also onε; it is therefore obvious that when $N(M-1) > \varepsilon$, this regime does not exist.

All the expressions of convection thresholds are seen to vary proportionally with Ha inducing a monotonous increase of these thresholds by increasing this parameter. Thus, the magnetic buoyancy force, induced by the introduction of an external magnetic field, has a stabilizing effect characterized by a delay of the onset of the convective flows.

7. COMPARISON OF THE PRESENT RESULTS WITH PREVIOUS ONES

The obtained analytical solutions and linear stability analysis results are compared with those reported earlier by Rakoto Ramambason and Vasseur (2007)who studied the influence of the magnetic field on Soret convection in shallow Darcy porous horizontal enclosure. Their results, which correspond to the case where zero mass flux $(j' = 0)$is imposed on the horizontal boundaries, can be deduced from the present study by using the limits$N: \to 0$, $NM \to -\varphi$ and $Da \to 0$. For these limits, the expressions of ψ, T, S, Nu and Sh, obtained from Eqs.(8)-(10) and Eqs. (14)-(15), are :

$$\psi(y) = \psi_0(1-4y^2)$$

$$T(x,y) = C_T x - y - C_T\psi_0\left(\frac{4}{3}y^3 - y\right)$$

$$S(x,y) = C_S x - \psi_0(LeC_S + C_T)\left(-\frac{4}{3}y^3 + y\right) - y$$

$$Nu = \frac{45+24{\psi_0}^2}{45+4{\psi_0}^2}$$

$$Sh = \frac{45+24Le^2{\psi_0}^2}{45+4Le^2{\psi_0}^2}$$

The corresponding thresholds of convection are deduced from the results obtained using the parallel flow approach (Eqs.(17)-(18)) or from those based on the linear stability analysis (Eqs. (38)-(39)) as:

$$R_{TC}^{sup} = \frac{12(1+Ha^2)}{(1+(1+Le)\varphi)}$$

$$R_{TC}^{sub} = \frac{(1+Le)(1+Ha^2)}{Le^5} R^{sup}[(Le-1)(Le - \varphi) - \varphi(1+Le) + 2\sqrt{\varphi Le^2(\varphi - Le - 1)}]$$

The above expressions obtained for ψ, T, S, Nu, Sh, R_{TC}^{sup} and R_{TC}^{sub} are identical to those reported by Rakoto Ramambason and Vasseur (2007).

Also, the results obtained by Bahloul *et al*. (2003), while studying double-diffusive and Soret-induced convection in a shallow horizontal porous layer in the absence of magnetic field are deduced successfully from the present study, by using the limits $N \to 0$, $NM \to -\varphi$,$Ha \to 0$ and $Da \to 0$. Particularly, the expression of the threshold of oscillatory convection is deduced from the present solution as:

$$R_{TC}^{Hopf} = \frac{(\varepsilon Le + 1)}{Le(\varepsilon + \varphi)} R^{sup}$$

Isidentical to the one reported by Bahloul *et al*. (2003).

8. RESULTS AND DISCUSSION

8.1 Stability Diagram

The stability diagram, presented in Fig. 3 for $Le = 10$, $M = 0.5$ and $\varepsilon = 0.5$ is used to analyze the flow behavior and the nature of the bifurcations. In the figure, the different regions are delineated by the thresholds of subcritical, Hopf and stationary convection, in which different flow behaviors may occur. The stability diagram is presented in the(R_{TC}^0, N)plane with$R_{TC}^0 = R_{TC}/((1+Ha^2)R^{sup})$. The Rayleigh number is scaled by the parametersR^{sup} and Ha such that the diagram remains valid for any Darcy and Hartmann numbers. The linear stability analysis indicates that the wave number is zero; hence, only mono-cellular flows prevail. Region (A) describes an unconditionally stable motionless state in which any dynamic perturbation (regardless its amplitude) decay with time. Region (B) delineates possible subcritical convection, in which the rest state instability can be triggered only by large finiteamplitude perturbations. The sub-codimension-2 point (the intersection between the thresholds of subcritical and stationary convection) results from the merging of subcritical and stationary bifurcations saddle-node points and is given by the following coordinates:

$$\left.\begin{aligned} N^{sub-c2} &= \frac{1}{(M-1)Le^3 + MLe^2 + MLe + M} \\ R_T^{0,sub-c2} &= \frac{(M-1)Le^3 + MLe^2 + MLe + M}{(M-1)Le^3 + MLe^2 + Le} \end{aligned}\right\} \quad (40)$$

Region (B) extends to the upper limit delineated by the dashed-line, where the onset of oscillatory convection (Hopf's bifurcation) occurs. In the close vicinity of the Hopf's bifurcation threshold,R_{TC}^{Hopf}, any perturbation (regardless of its amplitude) will grow in time in an oscillatory manner. Therefore, in region (C), sustained oscillatory or steady convection is possible. Furthermore, within this region, strong perturbations may cause the flow to bifurcate towards a steady state. The Hopf-codimension-2 point is indicated on the stability diagram, and its coordinates are given by the following, by equating the critical Rayleigh numbers expressions obtained for Hopf and stationary bifurcations:

$$\left.\begin{aligned} N^{Hopf-c2} &= \frac{1}{(M-1)\varepsilon Le^2 + M\varepsilon Le + M} \\ R_T^{0,Hopf-c2} &= \frac{(M-1)\varepsilon Le^2 + M\varepsilon Le + M}{(M-1)\varepsilon Le^2 + (M(\varepsilon-1)+1)Le} \end{aligned}\right\} \quad (41)$$

In region (D), the fluid is unconditionally unstable and the bifurcation occurs via a stationary convection.

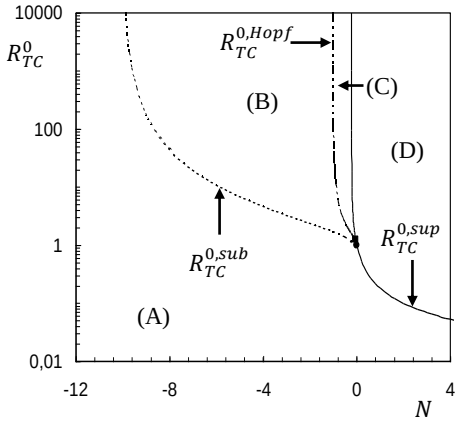

Fig. 3. Stability diagram for $Le = 10$, $M = -0.5$ and $\varepsilon = 0.5$.

8.2 Effect of Hartmann Number Ha

The Hartmann number,Ha, is a measure of the magnetic buoyancy force. It could be varied by changing the strength of the magnetic field or by considering various working electrically conducting fluids or different porous media with different permeability. A good assessment of the interaction between the applied external magnetic field and the resulting heat and mass transfer is necessary for an appropriate control of thermomagnetic devices. Figure 4 (a)-(c) shows the evolutions of the flow intensity,ψ_0, the Nusselt number, Nu, and the Sherwood number, Sh, with Ha for $R_T = 200$, $Da = 0.01$, $M = 0.5$, $Le = 10$, $N = 0.5$ and $N = -0.75$. It is noticed that the solutions presented here are those corresponding to positive and negative signs within the square root in Eq. (16). The ones corresponding to negative sign were not obtained numerically despite the multiple trials performed using different initial conditions(including the analytical solution itself). Therefore, in the following discussion, the solutions with positive and negative signs within the square root in Eq. (16) will be termed as stable and unstable branches, respectively. The analytical solutions for ψ_0, Nu and Sh, corresponding to the stable branches are seen to be in good agreement with the numerical results. A close inspection of the results, presented in these figures, shows clearly that the magnetic field has

a strong effect on flow characteristics and heat and mass transfer. The case of subcritical convection is illustrated in Figs. 4(a)-(c) for $N = -0.75$, for which both stable and unstable branches exist for$0 \leq Ha \leq Ha_{c1} = 2.765$. For the stable branch, the increase of Ha induces a decrease of the quantitiesψ_0 and Nu indicating that the magnetic field reduces the flow intensity and the heat transfer rate. However, the evolution of Sh in the range$0 \leq Ha \leq Ha_{c1}$ exhibits a different behavior characterized by an increase towards a maximum value $Sh_{max} \cong 7.567$ at$Ha_{max} = 1.42$ then by a decrease (in a very small range of Ha) before the disappearance of the stable branch. For the unstable branch the quantitiesψ_0, Nu and Sh are observed to increase by increasing Ha and this branch vanishes for $Ha > Ha_{c1}$.

The case of supercritical convection is given in Figs.4(a)-(c) for $N = 0.5$ for which an increase of Ha from 0 to $Ha_{c2} = 6.97$ induces a decrease of the quantitiesψ_0 and Nu indicating that the magnetic field reduces the flow intensity and the heat transfer. However, the evolution of Sh in the range$0 \leq Ha \leq Ha_{c2}$ exhibits a different behavior characterized by an increase towards a maximum value$Sh_{max} \cong 7.689$at$Ha_{max} \cong 1.6$then by a decrease towards $Sh = 2$. In fact, for$Ha = Ha_{c2}$, the Sherwood number becomes equal to $Sh = 1/(1 - M)$, which explains the value of Sh obtained for $M = 0.5$. The critical value of Ha can be computed by the following expression:$Ha_{c2} =$

$$\left[-1 + (1 + NLe - (1 + Le)NM)\left(\frac{R_T}{R^{sup}}\right)\right]^{\frac{1}{2}} \quad (42)$$

By increasingHa, the magnetic force overcomes the destabilizing force(s) effect and leads to a suppression of the convective flow. It appears clear from Eq. (42), that it is possible to predict the critical magnetic field necessary to suppress convection motion if the fluid properties and their dependence on temperature and solute concentration are known. These behaviors observed under the influence of an external magnetic field can be explained by the competition between the destabilizing effect of the thermal buoyancy force, the stabilizing effect of the magnetic force and the stabilizing ($N < 0$) or destabilizing ($N > 0$) effect of the solutal buoyancy force. This explains why a supercritical convection persists a long time($Ha_{c1} < Ha_{c2}$) in comparison with the subcritical one, before its disappearance under the effect of an external magnetic field. As known, for such flow configuration convective boundary layer regime does not exist as the convective flow is normal to the gravity. Obviously, short hydrodynamic boundary layers can form along the vertical boundaries for high Rayleigh numbers.

Also, for that specific value of the Rayleigh number and other chosen controlling parameters, pseudo-conduction is not possible as subcritical finite amplitude convection prevails. This phenomenon can be observed for the unstable solution but it is not physical.

9. CONCLUSION

The effect of an applied magnetic field on the Soret natural convection, developed in a horizontal layer heated and salted from below with constant heat and mass fluxes is conducted analytically and numerically. The thresholds for subcritical, oscillatory and stationary convection are obtained explicitly as functions of the governing parameters. The existence of a codimension-2 point is demonstrated and different flow regimes are delineated. The introduction of magnetic buoyancy forces has a stabilizing effect on the system; it leads to a reduction of the flow intensity and heat transfer. However, it can induce an increase or a reduction of the mass transfer rate; depending on the values of Ha. The external magnetic field makes possible the control of convective flows for an electrically conducting binary mixture saturating a porous layer.

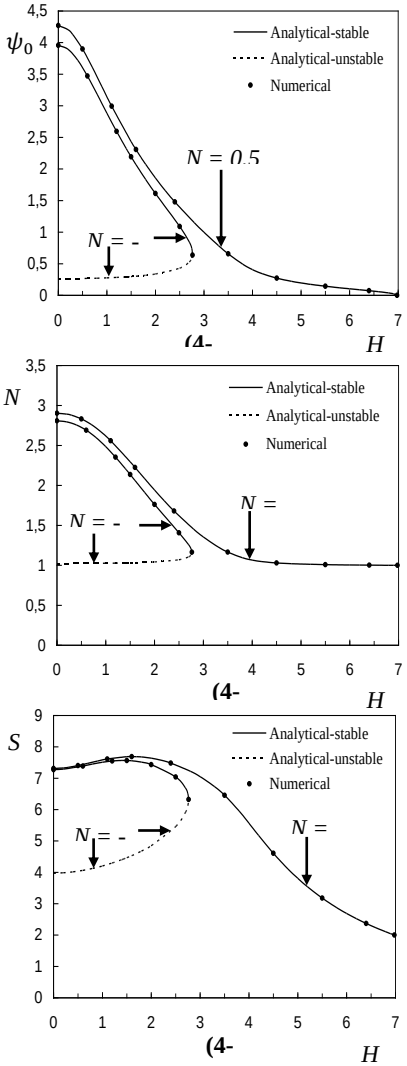

Fig. 4(a)-(c). Effect of Ha on (a) ψ_0, (b) Nu and (c) Sh for $R_T = 200$, $Da = 0.01$, $M = 0.5$, $Le = 10$, $N = 0.5$ and $N = -0.75$.

REFERENCES

Alvesa, S.I., A. Bourdonb and A. M. FigueiredoNetoa (2005).Investigation of the Soret coefficient in magnetic fluids using the Z-scan technique.*Journal of Magnetism and Magnetic Materials 289, 285-288.*

Bahloul, A., N. Boutana and P. Vasseur (2003).Double-diffusive and Soret-induced convection in a shallow horizontal porous layer.*J.Fluid. Mech 491, 325-352.*

Blums, E. (2005). New transport properties of ferrocolloids: magnetic Soret effect and thermomagnetoosmosis. *Journal of Magnetism and Magnetic Materials 289, 246-249.*

Blums, E., A. Mezulis, M. Maiorov and G. Kronkalns(1997). Thermal diffusion of magnetic nanoparticles in ferrocolloids: experiments on particle separation in vertical columns. *Journal of Magnetism and Magnetic Materials 169, 220-228.*

Blums, E., S. Odenbach, A. Mezulis and M. Maiorov (1998).Soret coefficient of nanoparticles in ferrofluids in the presence of a magnetic field.*Physics of Fluids 10, 2155-2163.*

Bourich, M., M. Hasnaoui and A. Amahmid (2003). A Soret effect on thermosolutal convection developed in shallow porous cavity: analytical and numerical study. *In Proceedings of Current Issues on Heat and Mass Transfer in Porous Media, Black sea, Romania*.

Bourich, M., Hasnaoui,M. M. Mamouand A. Amahmid(2004).Soret effect inducing subcritical and Hopf bifurcations in a shallow enclosure filled with a clear binary fluid or a saturated porous medium: a comparative study. *Physics of Fluids 16, 551-568.*

Braithwaite, D., E. Beaugnon and R. Tournier (1991).Magnetically controlled convection in a paramagnetic fluid.*Nature 354, 134-136.*

Cormack, D.E.,L. G. Leal and J. Imberger (1974). Natural convection in a shallow cavity with differentially heated end walls, part 1: asymptotic theory. *Journal of Fluid Mechanics 65, 209-230.*

Ece, M. C. and E. Büyük (2005). Natural convection flow under a magnetic field in an inclined rectangular enclosure heated and cooled on adjacent walls. *Fluid Dynamics Research 44, 933-943.*

Gaikwad, S. N. and S. S. Kamble (2014). Linear stability analysis of double diffusive convection in a horizontal sparsely packed rotating anisotropic porous layer in presence of Soret effect. *Journal of Applied Fluid Mechanics 3, 459-471*.

Gangadhar, K. (2013). Soret and Dufour effects on hydro magnetic heat and mass transfer over a vertical plate with a convective surface boundary condition and chemical reaction.*Journal of Applied Fluid Mechanics 6, 95-105.*

Jana, S., S. Dost V. Kumar and F. Durst (2006). A numerical simulation study for the Czochralski growth process of Si under magnetic field.*International Journal of Engineering Science 44, 554-573.*

Kaneda, M., T. Tagawa and H. Ozoe (2005). Natural convection of liquid metal under a uniform magnetic field with an electric current supplied from outside. *Experimental Thermal Fluid Science 30, 243-252.*

Mamou, M., P. Vasseur and M. Hasnaoui (2001).On numerical stability analysis of double-diffusive convection in confined enclosures.*Journal of Fluid Mechanics 433, 209-250.*

Mezulis, A. and E. Blums (2003).Two-dimensional determining of the transport coefficients under an applied magnetic field.*Magnetohydrodynamics 39, 369-375.*

Odenbach, S. and T. h. Völker (2005).Thermal convection in a ferrofluid supported by thermodiffusion.*J. Magnetism Magnetic Materials 289, 122-125.*

Pal, D. N. and H. Mondal (2013). Influence of Soret and Dufour on MHD buoyancy-driven heat and mass transfer over a stretching sheet in porous media with temperature-dependent viscosity. *Nuclear Engineering and Design 256, 350-357.*

Pal, D. N. and H. Mondal (2014).Soret-Dufour effects on hydromagnetic non-Darcy convective-radiative heat and mass transfer over a stretching sheet in porous medium with viscous dissipation and ohmic heating. *Journal of Applied Fluid Mechanics 7, 513-523.*

RakotoRamambason, D.S. and P. Vasseur (2007). Influence of a magnetic field on natural convection in a shallow porous enclosure saturated with a binary fluid.*ActaMechanica 191, 21–35.*

Roache, P.J. (1982). *Computational fluid dynamics*.Hermosa Publishers, Albuquerque, NM.

Shercliff, J.A. (1965). *A textbook on magnetohydrodynamics.*Pergamon Press Oxford.

Völker, T. H. and S. Odenbach (2005).Thermodiffusion in ferrofluids in the presence of a magnetic field.*Physics of Fluids 17, 037104.1-037104.6.*

Völker, T. H. and S. Odenbach (2005).Thermodiffusion in Magnetic fluids.*Journal of Magnetism and Magnetic Materials 289, 289-291.*

Völker, T. H., E. Blums and S. Odenbach (2004). Determination of the Soret coefficient of magnetic particles in a ferrofluid from the steady and unsteady part of the separation curve.*Int. J. Heat Mass Transfer 47, 4315-4325.*

Xu, B., B. Q. Li and D. E. Stock (2006).An experimental study of thermally induced convection of molten gallium in magnetic fields.*International Journal of Heat Mass Transfer 49, 2009-20*